J. Fluid Mech. (1995), *vol.* 292, *pp.* 325–332

The rise velocity and shape of bubbles in pure water at high Reynolds number

By P. C. DUINEVELD

J.M. Burgers Centre for Fluid Mechanics, Department of Applied Physics, University of Twente, PO Box 217, 7500 AE Enschede, The Netherlands

(Received 23 February 1994 and in revised form 5 January 1995)

The velocity and shape of rising bubbles, with an equivalent radius of 0.33-1.00 mm, in 'hyper clean' water, have been experimentally determined. For the small bubbles there is perfect agreement with theory, proving that this water can be considered as pure (no surfactants). For the larger bubbles there is a small discrepancy due to an overestimation in the theory.

1. Introduction

In this paper we report on the velocity of rise of slightly deformed bubbles in water. These bubbles have Reynolds numbers of $O(10^2)$, Weber numbers of $O(1)$ and can approximately be described as oblate spheroids. Here the Reynolds number and the Weber number are defined as $Re = 2UR/\nu$, and $We = 2\rho U^2 R/\sigma$, respectively, where ν and ρ denote the kinematic viscosity and density of the liquid, σ the surface tension, R the equivalent radius of the bubble and U the bubble rise velocity.

An outstanding contribution to the theory of bubble motion at high Reynolds numbers was given by Levich (1949, see also Levich, 1962), who calculated the drag of a spherical bubble from the dissipation in the liquid, as given by potential flow theory. Moore (1963, 1965), extended this result to higher-order in the Reynolds number and included the deformation of the bubbles. Moore calculated the deformation of the oblate spheroidal bubble in an approximate way by equating the normal force balance only at a few points on the bubble surface. El Sawi (1974) and Benjamin (1987) satisfied this boundary condition on the complete bubble surface. Miksis, Vanden-Broeck & Keller (1981) calculated the bubble shape by a numerical method and allowed for a deviation from the oblate spheroidal shape. In these three articles potential theory was used, resulting in bubbles with fore-aft symmetry, and no steady axisymmetric bubble shape was found above a Weber number of 3.2.

Ryskin & Leal (1984) numerically calculated drag coefficients and bubble shapes as a funcion of the Weber number for various Reynolds numbers. For large Reynolds numbers and even at small Weber numbers fore-aft symmetry no longer holds, resulting in a somewhat different drag coefficient than given by Moore (1965). Owing to numerical problems the authors were limited to a maximum Reynolds number of 200, corresponding to a bubble with $R = 0.45$ mm in water.

Extensive experiments were carried out by Haberman & Morton (1954), who measured rise velocities as a function of bubble size for various liquids. Saffman (1956) and Hartunian & Sears (1957) both report on experiments and theory dealing with path instability of a rising bubble.

All these authors noticed the influence of surface-active impurities on the rise velocity. Water, especially, is very sensitive to such impurities; even distilled water is not perfectly pure, as was found by Aybers & Tapuccu (1969). Yet pure water is of importance, because it is a liquid with an extremely low Morton number. This Morton number depends on the liquid properties only and is defined as $M = g\mu^4/\rho\sigma^3$, where g is the acceleration due to gravity. Water at 20 °C has a value of 2.4×10^{-11}. In a liquid with a low Morton number, bubbles rising at large Reynolds numbers will have reasonably small deformation. These bubbles are essential to test the theories mentioned here.

So the question arises of whether water can be so clean that there is no influence of impurities on the rise velocity. This is the subject of this paper. We have measured rise velocities and shapes of bubbles in 'hyper clean' water. Our measurements fill a gap, noticed by Ryskin & Leal (1984), concerning bubbles with high Reynolds and low Weber numbers. Here R was varied between 0.33 and 1.00 mm. For the small bubbles there is a perfect agreement with theory, proving that our water can be considered as pure (no surfactants). For the larger bubbles there is an increasing deviation from theory, which is due to an overestimation of the deformation in the theories mentioned. Our measurements of the shapes of the larger bubbles show that the bubble no longer exhibits fore-aft symmetry, contrary to what is assumed in the theories.

2. Experimental method

The experiments were performed in a cubic tank with glass walls of 50 cm length. The tank was filled with 'hyper clean' water, produced with a Millipore purification system. The quality after purification was: specific resistance 18.2 MΩ cm and less than 10 p.p.b. organic particles. The temperature of the water during all experiments was 19.6 ± 0.2 °C.

Bubbles were produced very accurately with a specially designed system, described in detail by Kok (1993). Bubbles sizes were obtained by measuring the length of the air plug in the feed capillary. The equivalent radius was varied between 0.33 and 1.0 mm, with a relative error between 0.8% for $R = 0.33$ and 0.3% for $R = 1.0$ mm. This error is caused by a measuring fault in the length of the air plug and the diameter of the capillary.

The motion was recorded with a NAC HSV-1000 high speed video with 500 frames s^{-1}, loaded with a Fuji S-VHS video tape. Back lighting was provided by two stroboscopes with a flash pulse of less than 10 μs. The camera was equiped with a Canon Zoom lens f/1.6 16–108 mm with a diaphragm f:5.6, a Canon extender 2× and a messing extension ring of 17 mm. The images were digitized into 768×512 pixels, with 8 bit grey level resolution, by a VFG Variable Scan Framegrabber (Imaging Technology Inc.)

The centre and the shape of the bubble projection were determined with image software routines. The bubble contour $r(\theta)$ is a periodic function of θ with period 2π and can be written as

$$r(\theta) = A_0 + \sum_{n=1}^{N} A_n \cos n\theta + \sum_{n=1}^{N} B_n \sin n\theta. \tag{2.1}$$

A_n and B_n can be determined with Fourier transform methods. An accurate description of the shape could be obtained with a number of modes typically less than 8. Also,

by not including higher-order terms, noise, due to the finite resolution of the system, is eliminated. The deformation of the bubble, χ, is the ratio between the longer and smaller axes. The longer axis can be found from

$$L - A_0 = max \left\| \sum_{n=2}^{N} (A_n \cos n\theta + B_n \sin n\theta) \right\|. \tag{2.2}$$

Solving this equation gives the angle θ_m between the longer and θ axes. The smaller axis is found from $\theta_m + \pi/2$.

3. Experimental results and discussion

3.1. *Rise velocities*

The measured rise velocities are compared with the velocities determined by the expression for the drag coefficient as given by Moore (1965),

$$C_D = \frac{48G(\chi)}{Re}\left(1 + \frac{H(\chi)}{Re^{1/2}} + \ldots\right), \tag{3.1}$$

valid for high Reynolds numbers. Here $G(\chi)$ and $H(\chi)$ are functions of the deformation χ, with $G(\chi)$ given by

$$G(\chi) = \tfrac{1}{3}\chi^{4/3}(\chi^2 - 1)^{3/2}\frac{(\chi^2 - 1)^{1/2} - (2 - \chi^2)\sec\chi^{-1}}{\left(\chi^2 \sec\chi^{-1} - (\chi^2 - 1)^{1/2}\right)^2}, \tag{3.2}$$

and $H(\chi)$ as follows from table 1 in Moore (1965).

The deformation is found from the relation between the Weber number and χ, where the approximate relation given by Moore (1965), is used,

$$W(\chi) = 4\chi^{-4/3}(\chi^3 + \chi - 2)\left[\chi^2 \sec\chi - (\chi^2 - 1)^{1/2}\right]^2 (\chi^2 - 1)^{-3}, \tag{3.3}$$

because for χ less than 2 there is no noticeable difference with the exact relation of Benjamin (1987) and El Sawi (1974).

The rise velocity of a bubble is not immediately constant, but grows from zero at release to its final value. From a force balance it can be shown that this distance travelled is at most 0.07 m for bubbles in our experiment.

In figure 1 the experimentally determined rise velocities are plotted as a function of R and compared with the theoretical curve. The bubbles were recorded at a distance of 10 to 12 cm from the release point. Rise velocities in this range proved to be perfectly stationary and errors are small, at most 0.3 cm s^{-1}.

In the range $R \approx 0.4$ to 0.6 mm there is good agreement between theory and experiment. For smaller sizes the measured velocities are somewhat lower than theoretical values, because for these bubbles the neglected term in (3.1) gives a small, but noticeable, contribution. For a spherical bubble this term is of order $Re^{-5/6}$. For the larger bubbles this contribution is of smaller order than the error caused by the uncertainty in the bubble size. Ryskin & Leal (1984) calculations included drag coefficients for bubbles with $Re = 100$ and 200, as a function of the Weber number. From their results we find for a bubble with $R = 0.36$ mm a rise velocity of 15.7 ± 0.2 cm s^{-1}, in good agreement with the experimental velocity of 15.3 ± 0.2 cm s^{-1}. Above $R = 0.6$ mm the experimental rise velocity is slowly becoming larger than the theoretically determined one, but the shapes of the two curves are more or less similar. In the next section we discuss this difference in more detail.

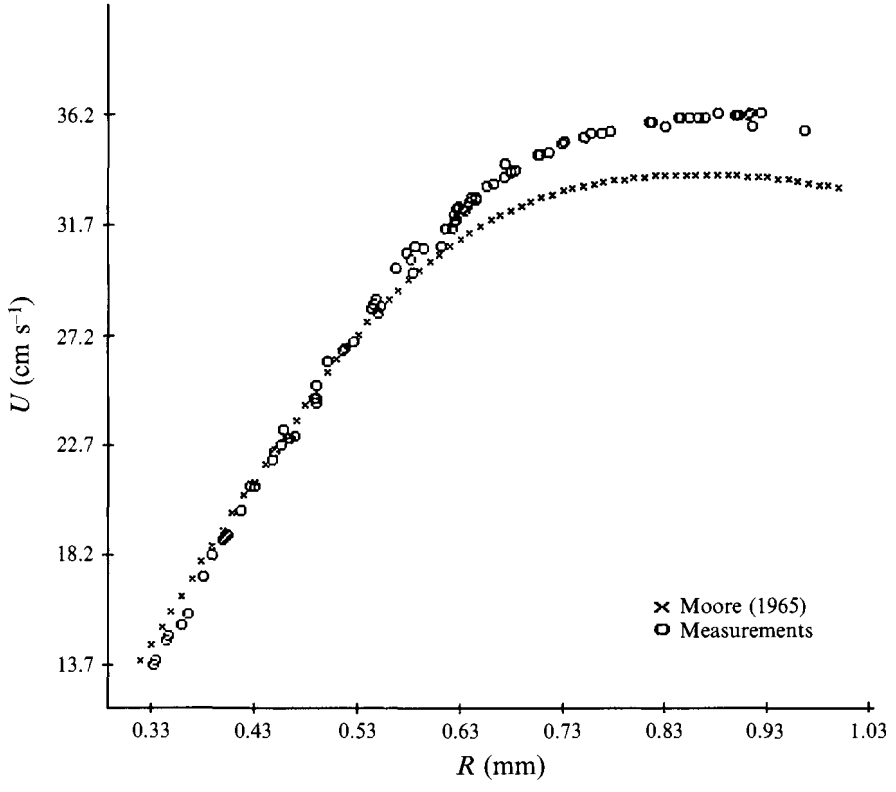

FIGURE 1. Vertical rise velocity of a bubble in pure water.

To the best of my knowledge the measured rise velocities are the largest ever measured. In particular, the velocity of the small bubbles proves to be larger than in previous experiments. Kok (1993) reports a rise velocity of 0.236 m s^{-1} for a bubble with $R = 0.5$ mm. Aybers & Tapuccu (1969) measured rise velocities for different bubble sizes as a function of the distance travelled. Their results show a maximum rise velocity and after that a decrease with the distance travelled. This decrease was relatively large for small bubbles and small for large bubbles, clearly indicating the existence of surface-active impurities. The experimental results of Haberman & Morton (1954) also show a relatively large difference between the experimentally and theoretically determined rise velocity for small bubbles and a small difference for large bubbles. Hence distilled water contains a noticeable amount of surface-active impurities, which have a larger influence on small bubbles than on larger bubbles. This qualitative picture also follows from the theoretical work of He, Maldarelli & Dagan (1991) for bubbles in Stokes flow.

In all our measurements rise velocities were stationary and equal to or larger than values predicted by theory, so we conclude that for the bubble sizes in this work the 'hyper clean' water can be considered as pure (no surfactants).

3.2. *Bubble shapes*

We have mentioned a difference between the theoretical and the experimental rise velocity above $R \approx 0.6$ mm. By considering in more detail the shape of the bubble the cause of this becomes clear.

The equation for the bubble deformation (3.3) is based on potential flow theory,

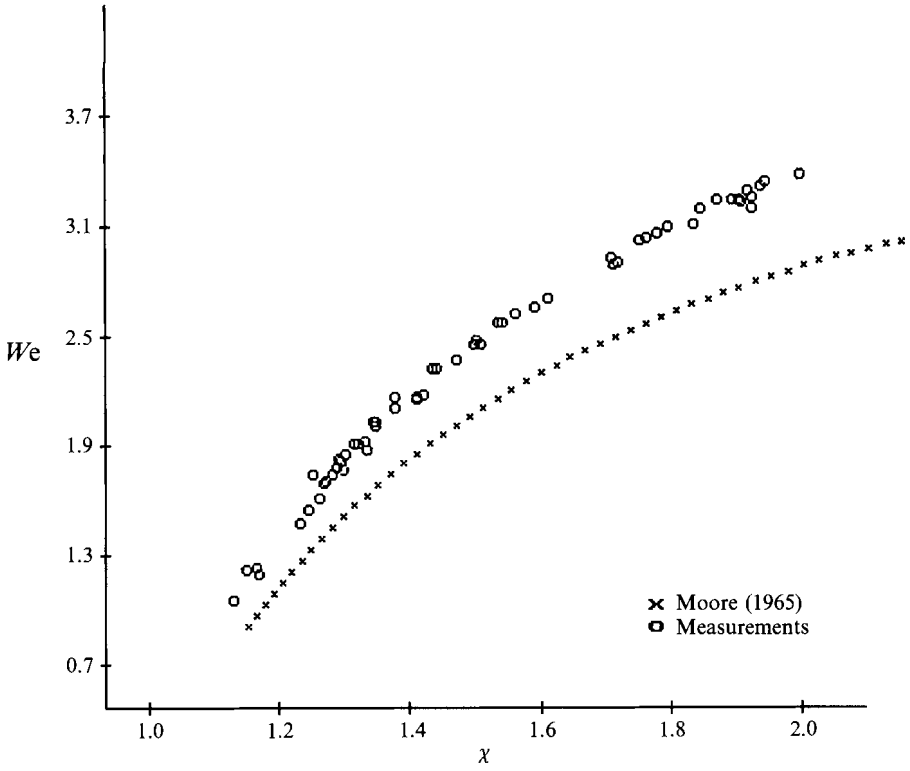

FIGURE 2. Theoretical and experimental determination of We as a function of χ.

which leads to a fore-aft symmetry and an axial symmetry of the bubble. In figure 2 we have plotted the experimental and theoretical Weber number against the deformation of the bubble, for $R > 0.53$ mm. For small bubbles there is a reasonable agreement between theory and experiment, but for larger bubbles there is an increasing deviation caused by theoretical overestimation of the deformation, which is also shown in figure 3. This overestimation of the deformation causes the theoretical rise velocity to be lower than observed. If the experimental fit for the deformation is used in the theoretical calculation of the rise velocity, it can be shown that theory and experiment are in agreement. Note here that for the small equivalent bubble radii there is a noticeable difference between the experimentally and theoretically determined deformation. However the rise velocities in this range are equal. Apparently the overestimation of the deformation cancels with the contribution from the neglected term in (3.1).

We now discuss in more detail the observed bubble shapes, more specifically the number of terms in (2.1) necessary for a reasonable description of the bubble contour. In figure 4, two different bubble sizes are shown, $R = 0.64$ and $R = 0.91$ mm. A bubble with $R = 0.64$ mm can well be described by the first two terms ($n = 0, 2$) and fore-aft symmetry holds; however for $R = 0.91$ mm terms up to $n = 8$ are required and this contour shows a deviation from fore-aft symmetry. This deviation starts at $R \approx 0.6$ mm and grows with increasing bubble size. At the point where agreement between theory and experiment in figure 1 is lost ($R \approx 0.6$ mm), fore-aft symmetry no longer holds as well.

When fore-aft symmetry is lost the front of the bubble becomes flatter than the

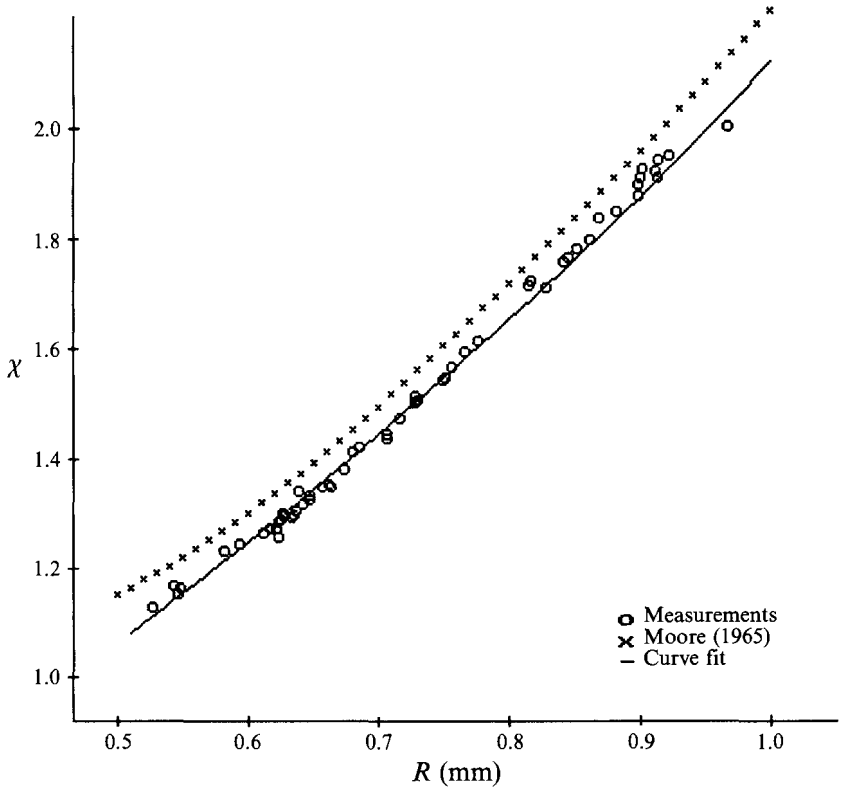

FIGURE 3. Theoretical and experimental determination of χ as a function of the equivalent bubble radius.

rear (figure 4*d*), in qualitative agreement with the numerical results of Ryskin & Leal (1984). They show this to be caused by a standing eddy behind the bubble. Our experimental bubble shape gives indirect support for this standing eddy, but no direct comparison can be made, because here Reynolds numbers are larger than studied by Ryskin & Leal.

3.3. *Path instability*

At $R = 0.91$ mm and an associated Weber number of 3.3 a path instability occurs: i.e. the bubble starts to zigzag. The cause of this path instability is not yet clear. From the work of Ryskin & Leal (1984) and Leal (1989) it is at the moment believed to be due to shedding of vortices. For this to happen a standing eddy must exist behind the bubble. The authors showed that this eddy is not created by boundary layer separation, as is the case for a solid sphere, but by an accumulation of vorticity at the rear of the bubble. An indication of this eddy may be found in figure 4(*d*).

The bubble size and the Weber number at the onset of path instability are nearly equal to the experimentally determined result of Hartunian & Sears (1957), $We = 3.2$. This is in contradiction with the suggestion of Ryskin & Leal (1984) that path instability will occur for $We \sim 5$. They base this on measurements of Tsuge & Hibino (1977), who found critical Weber numbers of about 5 for highly purified alcohols. The difference with Hartunian & Sears was believed by Ryskin & Leal (1984) to be due to surface-active impurities. However in our experiments the water is pure and

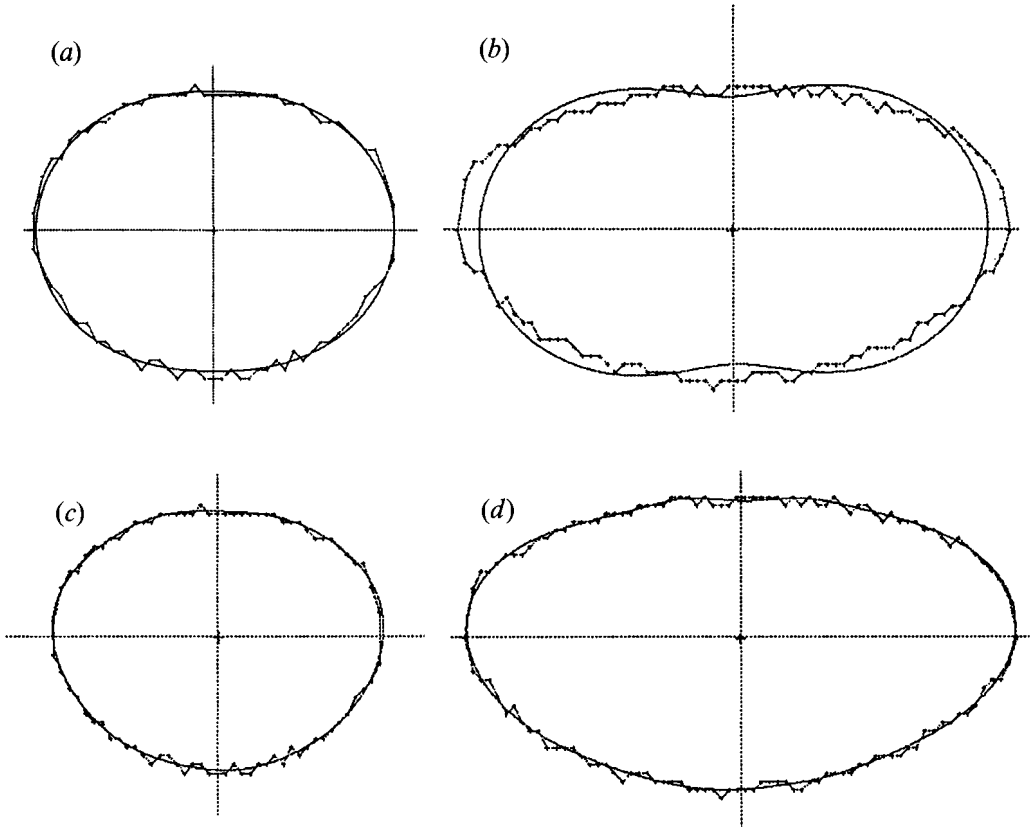

FIGURE 4. Bubble contour, fitted with terms up to $n = 2$: (*a*) $R = 0.64$ mm; (*b*) $R = 0.91$ mm. Bubble contour, fitted with terms up to $n = 8$: (*c*) $R = 0.64$ mm; (*d*) $R = 0.91$ mm.

still a nearly similar result is found. The reason for the difference in critical Weber number is that this number depends on the Morton number, as follows from Tsuge & Hibino (1977). They found that water, which has a lower Morton number than purified alcohols, will have a lower critical Weber number. Our pure water data are in good agreement with the empirical relation of Tsuge & Hibino (1977). The good agreement between our results and those of Hartunian & Sears (1957) shows that distilled water can be considered as nearly clean for *this* bubble size (not for small bubbles).

Saffman (1956) found the onset of path instability to occur at $R = 0.7$ mm. The difference with our experiment is probably due to impurities in the water used by Saffman. From the work of Hartunian & Sears it follows that path instability occurs at a lower Reynolds number if the liquid contains impurities.

In the calculations of Miksis *et al.* (1981), El Sawi (1974) and Benjamin (1987) a maximum in the We–χ curve was found at $We = 3.2$. Steady bubble shapes above this Weber number are not possible according to these theories, hence $We \sim 3.2$ is the onset for shape instability. It is tempting to identify, as El Sawi (1974) did, the onset of path instability with the onset of shape instability. However, from our results of figure 2 it follows that the Weber number has certainly not attained its maximum. Therefore, the agreement between the experimentally determined Weber number for path instability and the theoretically determined Weber number for shape instability is pure coincidence, caused by theoretical overestimation of the deformation.

I would like to thank Professor L. van Wijngaarden for many helpful discussions, my collegue A. A. Woering for helping me with the image analyses, and M. M. van den Berg, A. H. de Boer, P. J. T. Reinders and H. Westhuis for their assistance with the experiments.

REFERENCES

AYBERS, N. M. & TAPUCCU, A. 1969 The motion of gas bubbles rising through stagnant liquids. Wärme-und Stoffübertragung **2**, 118–128.

BENJAMIN, T. B. 1987 Hamiltonian theory for motion of bubbles in an infinite liquid. *J. Fluid Mech.* **181**, 349–379.

EL SAWI, M. 1974 Distorted gasbubbles at large Reynolds number. *J. Fluid Mech.* **62**, 163–183.

HABERMAN, W. L. & MORTON, R. K. 1954 An experimental study of bubbles moving in liquids. *Proc. ASCE* **387**, 227–252.

HARTUNIAN, R. A. & SEARS, W. R. 1957 On the instability of small gas bubbles moving uniformly in various liquids. *J. Fluid Mech.* **3**, 27–47.

HE, Z., MALDARELLI, C. & DAGAN, Z. 1991 The size of stagnant caps of bulk soluble surfactants on the interface of translating fluid droplets. *J. Colloid Interface Sci.* **146**, 442–451.

KOK, J. B. W. 1993 Dynamics of a pair of gas bubbles moving through liquid II. Experiment. *Eur. J. Mech.*, B/*Fluids* **4**, 541–560.

LEAL, L. G. 1989 Velocity transport and wake structure for bluff bodies at finite Reynolds number. *Phys. Fluids* A **1**, 124–131.

LEVICH, V. G. 1949 *Zhur. Eksp. i Teoret. Fiz.* **19**, 18.

LEVICH, V. G. 1962 *Physico Chemical Hydrodynamics.* Prentice Hall.

MIKSIS, J. M., VANDEN-BROECK, J. & KELLER, J. B. 1981 Axisymmetric bubble or drop in a uniform flow. *J. Fluid Mech.* **108**, 89–100.

MOORE, D. W. 1963 The boundary layer on a spherical gas bubble. *J. Fluid Mech.* **16**, 161–176.

MOORE, D. W. 1965 The velocity of rise of distorted gas bubbles in a liquid of small viscosity. *J. Fluid Mech.* **23**, 749–766.

RYSKIN, G. & LEAL, L. G. 1984 Numerical solution of free-boundary problems in fluid mechanics. Part 2. Bouncy motion of gas bubble through a quiscent liquid. *J. Fluid Mech.* **148**, 19–35.

SAFFMAN, P. G. 1956 On the rise of small air bubbles in water. *J. Fluid Mech.* **1**, 249–275.

TSUGE, H. & HIBINO, S. I. 1977 The onset of oscillatory motion of single gas bubbles rising in various liquids. *J. Chem. Engng Japan* **10**, 66–68.